NANO LETTERS

2008
Vol. 8, No. 8
2405-2409

Ultralow Loading Pt Nanocatalysts Prepared by Atomic Layer Deposition on Carbon Aerogels

Jeffrey S. King,[†] Arne Wittstock,[‡,§] Juergen Biener,[*,‡] Sergei O. Kucheyev,[‡] Yinmin M. Wang,[‡] Theodore F. Baumann,[‡] Sandeep K. Giri,[†] Alex V. Hamza,[‡] Marcus Baeumer,[*,§] and Stacey F. Bent[*,†]

Department of Chemical Engineering, Stanford University, 381 North South Mall, Stanford, California 94305, Lawrence Livermore National Laboratory, Nanoscale Synthesis and Characterization Laboratory, 7000 East Avenue, Livermore, California 94550, and Institut für Angewandte and Physikalische Chemie, Universität Bremen, Leobener Strasse NW2, 28359 Bremen, Germany

Received May 6, 2008; Revised Manuscript Received June 23, 2008

ABSTRACT

Using atomic layer deposition (ALD), we show that Pt nanoparticles can be deposited on the inner surfaces of carbon aerogels (CA). The resultant Pt-loaded materials exhibit high catalytic activity for the oxidation of CO even at loading levels as low as ~0.05 mg Pt/cm^2. We observe a conversion efficiency of nearly 100% in the 150−250 °C temperatures range, and the total conversion rate seems to be limited only by the thermal stability of the CA support in ambient oxygen. The ALD approach described here is universal in nature, and can be applied to the design of new catalytic materials for a variety of applications, including fuel cells, hydrogen storage, pollution control, green chemistry, and liquid fuel production.

Nanoparticle catalyst materials are an active area of research with the potential for high impact in applications such as chemical manufacturing, pollution control, green chemistry, liquid fuel production, and power generation.[1–3] Particular emphasis has recently been placed on the development of advanced catalysts and electrode materials for fuel cells through the incorporation of noble metal nanoparticles into high surface area carbon supports.[4–6] The loading of catalyst particles into carbon nanostructures can be performed by a variety of methods, including the impregnation and reduction of metal salts into a support structure or the electrochemical deposition of catalyst particles on the carbon material. One of the challenges associated with the design of these electrode materials has been the development of methods that can reduce the overall loading of the costly noble metal catalyst while retaining the high catalytic activity of the material.[7] For example, the economic viability of direct methanol fuel cells requires a reduction in Pt catalyst loading from current levels of 2−8 mg/cm^2 to below 1 mg/cm^2.[5]

Recently, atomic layer deposition (ALD) has been demonstrated to be an excellent method for uniformly coating the inner surfaces of porous nanostructures with a variety of materials.[8–12] ALD is a process that provides atomic level control of thin film growth using sequential, self-limiting surface reactions.[13] Since film growth is self-limiting for each deposition cycle, the ALD process can be used to deposit conformal films inside high aspect ratio structures. For example, ALD has been used to deposit both metals and metal oxides, such as ZnO, Al_2O_3, W, Cu, and Ru, inside nanoporous monoliths.[8–11] Our previous study[9] has also revealed that ALD allows one to control the morphology of the deposited metal, from discrete nanoparticles to formation of a continuous film, through the surface chemistry. While the growth of nanoparticles is undesirable for many applications, this discovery suggests great promise in the field of catalysis where it allows one to maximize the accessible surface area of the catalyst. In addition, due to the self-limiting nature of the process, ALD can be used to control the amount of catalyst deposited on the support material. Hence, the process is ideally suited to determine the lower limits of metal loading in a catalytically active system.

Here, we use ALD to fabricate Pt-loaded catalysts derived from carbon aerogels (CAs). Such CAs are unique porous materials that exhibit numerous exceptional properties,

* To whom correspondence should be addressed. E-mail: (S.F.B) sbent@stanford.edu; (M.B.) mbaeumer@uni-bremen.de; (J.B.) biener2@llnl.gov.
[†] Stanford University.
[‡] Lawrence Livermore National Laboratory.
[§] Universität Bremen.

10.1021/nl801299z CCC: $40.75
Published on Web 07/18/2008

including mechanical stability, continuous porosity, high surface area, and high electrical conductivity and, as such, are attractive platforms for incorporation of catalytic particles. Using the ALD process, we show that Pt nanoparticles can be deposited on the inner surfaces of CA monoliths, and that the resultant Pt-loaded materials (Pt-CA), even those with extremely low areal densities of Pt ($\sim$0.047 mg/cm^2), exhibit high catalytic activities for the oxidation of carbon monoxide.

The CA support was synthesized using a procedure described elsewhere.[14] The skeletal structure of the material consists of interconnected submicron-sized carbon ligaments that define a continuous macroporous network. Despite being macroporous, the CA support still exhibits appreciable surface area ($\sim$480 m^2/g) due to microporosity within the carbon ligaments. As-synthesized CA monoliths were mechanically thinned to form disks of approximately 1 cm diameter and 500 μm thickness.

Following a recipe from ref 15, we deposited Pt in CAs by ALD using the (methylcyclopentadienyl)-trimethylplatinum ($MeCpPtMe_3$, Strem Chemical Co)/oxygen (dry air) ALD process in a warm wall reactor with a wall temperature of 125 °C and a stage temperature of 320 °C. Since the Pt ALD temperature window is relatively narrow, it was important to ensure that the CA substrate was at the right temperature during deposition. To increase heat transfer from the stage to the CA, hot wall conditions were replicated by placing CA disks inside a machined Al container with a perforated lid. This container was then placed inside the reactor directly on the heated stage. Due to the relatively low vapor pressure of $MeCpPtMe_3$ ($\sim$800 mTorr at 65 °C)[16] and the tortuous porosity of the CA support, very long pulse and purge times were used to maximize penetration of the ALD precursors into and removal of byproducts out of the CA support. A single ALD cycle consisted of a 20 min $MeCpPtMe_3$ pulse followed by a 10 min N_2 purge, a 10 min dry air pulse, and a 10 min N_2 purge. With such long cycle times and elevated temperatures, it was important to ensure that the CA would not degrade under the ALD conditions. Thermogravimetric analysis (TGA) revealed that at 250 °C under a 50 sccm air atmosphere for 4 h, no mass loss was observed, and at 350 °C minimal mass loss was detected. In order to maximize precursor utilization, quasi-static conditions were used for the $MeCpPtMe_3$ pulses, during which the chamber, isolated from the vacuum line, was exposed to the heated precursor (65 °C) with a flow of 0.5 sccm N_2, resulting in a pressure increase rate of $\sim$40 mTorr/s. Standard flow conditions were used for air and N_2 pulses. As the focus of this work is on the ultralow loading regime, the CAs were exposed to 2, 5, and 10 ALD cycles.

After ALD coating, the distributions and morphologies of Pt nanoparticles in CAs were characterized with Rutherford backscattering spectrometry (RBS, with 2 MeV ^{4}He ions backscattered to 164°) and cross-sectional transmission electron microscopy (XTEM, Philips CM-300 FEG). A focused ion beam instrument was used to prepare XTEM cross-sections. To extract the depth profiles of the Pt atomic concentration from RBS spectra, we used the RUMP code[17] as described elsewhere.[11] Oxidation of carbon monoxide, a well-studied model reaction, was used to characterize the catalytic activity of the resulting structures.[18] The specific surface area (SSA) before and after coating was estimated based on the Brunauer−Emmett−Teller (BET) N_2 adsorption method.

Structural characterization reveals that ALD is an efficient method to deposit highly dispersed Pt nanoparticles on the inner surfaces of CA monoliths. Figure 1a shows a low-magnification XTEM image of a CA treated with 10 ALD cycles, illustrating the expected spongelike structure of the macroporous CA support. Figure 1 panels b, c, and d are higher magnification XTEM images of the Pt-CA composite taken at depths of $\sim$1, 5, and 10 μm below the surface, respectively. These images clearly show the formation of discrete Pt nanoparticles on the interior surface of the CA. The crystallinity of the Pt nanoparticles is confirmed by the high-resolution XTEM image shown in Figure 1e as well as by selected area diffraction pattern analysis (Figure 1e, inset). Aside from the deposited Pt nanoparticles, the morphology of the CA support is consistent with uncoated supports, indicating no significant changes after ALD.

Further analysis of XTEM images (Figure 1f) reveals that the average particle size decreases with increasing depth, from $\sim$4.2 nm at the CA monolith surface to $\sim$2.4 nm at a depth of 5 μm. Between 5 and 10 μm, the average particle size remains nearly constant ($\sim$2.3 nm), whereas the density of Pt nanoparticles slightly decreases (see below). Figure 1e also reveals the relatively narrow size distribution of the deposited Pt nanoparticles for all three depths studied (standard deviations of $\sim$ 1.4, 0.8, and 0.6 nm for 1, 5, and 10 μm below the surface, respectively). The depth dependence of Pt particle sizes revealed by Figure 1 indicates a nonideal ALD process. As discussed in detail elsewhere,[11] nonideal ALD behavior could be attributed to precursor reactivity and to processes of adsorption−desorption equilibrium of both precursor and reaction product molecules with the pore walls. Although only the 10 cycle Pt-CA sample was characterized by XTEM, similar results (except for the lower coverage) can be expected for the 2 and 5 cycle samples.

Attempts to determine the Pt loading using CO adsorption measurements were unsuccessful since the Pt amount was below the detection limits ($\sim 10^{-6}$ mol). Instead, RBS was used to quantify the near-surface sample composition (up to $\sim$6 μm from the surface). Depth profiles of the Pt concentration in CAs are shown in Figure 2, indicating that the concentration of Pt increases with increasing the number of ALD cycles. In addition, for all three cases (of 2, 5, and 10 cycles) a higher Pt concentration is observed at the monolith surface, which is in agreement with XTEM data. Surface concentrations of 8.3, 2.3, and 1.5 Pt at % were observed for the 10, 5, and 2 cycle Pt-CA, respectively. Concentrations of 2.0, 0.4, and 0.4 Pt at % were observed at a depth of 6 μm for the 10, 5, and 2 cycle Pt-CA, respectively. The greater difference between 5 and 10 cycle Pt-CA is attributed to the existence of an ALD incubation period and a resulting lower growth rate that is often observed during the first several cycles of Pt ALD.[15] Results from Figure 2 suggest

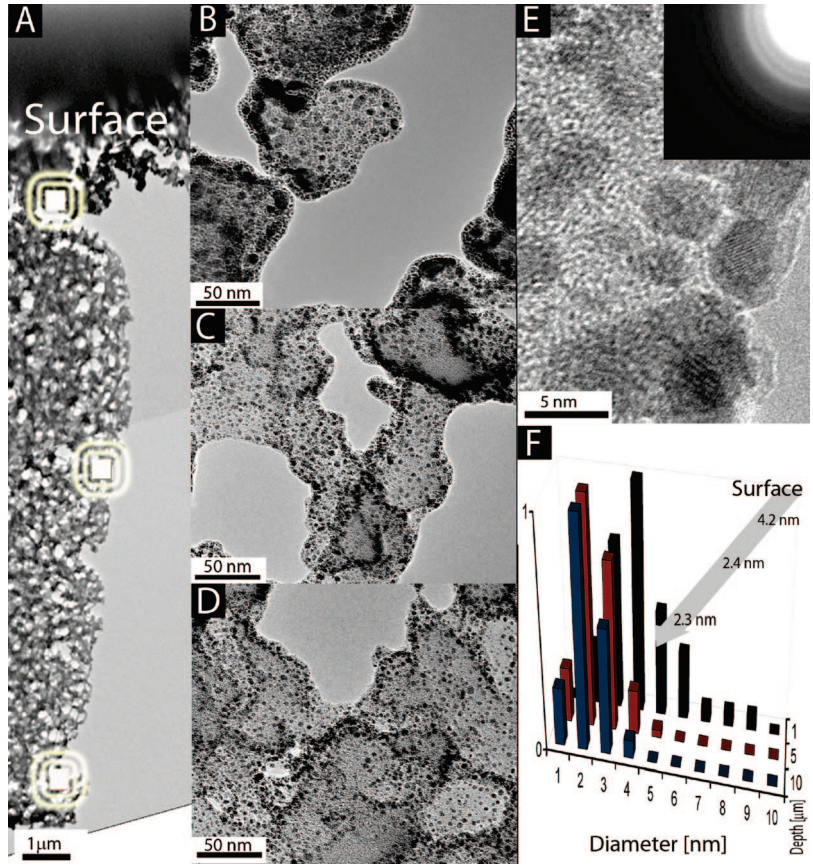

Figure 1. XTEM micrographs of a carbon aerogel treated with 10 Pt ALD cycles. (a) Low-magnification image. Higher magnification images taken from sample regions marked in panel a and corresponding to depths of (b) 1 μm, (c) 5 μm, and (d) 10 μm below the monolith surface with particle size histograms and resulting average particle diameter shown in (f). (e) High resolution image and a selected-area diffraction pattern in the inset indicating crystallinity of the ALD-deposited Pt nanoparticles at a depth of ~1 μm from the sample surface.

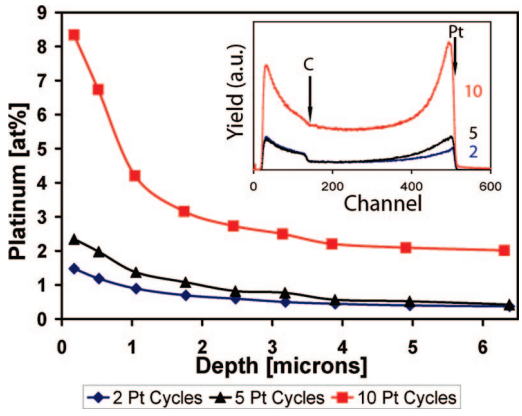

Figure 2. Depth profiles of the Pt concentration in a carbon aerogel infiltrated with 2, 5, and 10 Pt ALD cycles (as indicated in the legend) calculated from RBS spectra shown in the inset.

extremely low Pt loadings (i.e., the total weight of Pt atoms per area of the CA disk) of 0.26, 0.066, and 0.047 mg/cm^2 for the 10, 5, and 2 cycle Pt-CA, respectively. Our BET results also show that the SSA of Pt-CA composites slightly increases with the number of ALD cycles: 454, 593, and 626 m^2/g for the 2, 5, and 10 cycle samples, respectively. In view of the low Pt loading levels revealed by RBS, this increase in surface area is likely due to O_2 activation of the CA structure during the dry air portion of the ALD cycle. The increase in surface area is consistent with the previously discussed slight mass loss that was observed from TGA. However, it is important to emphasize that the Pt-CA samples were characterized after ALD, so any changes in the porosity and surface area that occurred in the deposition process are already taken into account in the subsequent catalytic analysis.

Despite their very low loading levels, the Pt-CA composite materials were found to be highly active as catalysts for CO oxidization. The catalytic activity of these materials was characterized in a continuous flow reactor constructed of glass tubing (see the inset in Figure 3b). The reactor was equipped with a glass frit in the lower section for supporting monolithic parts of the Pt-CA composites.[19] Gases were preheated by flowing them through a helical glass coil encircled reactor (30 cm height, 2 cm inner diameter) housed in a tube furnace. Dry synthetic air (80/20 vol % N_2/O_2) and CO were injected into the apparatus with a total gas flow of 50 sccm (mass flow controllers, Maettig Bronkhorst). The amount of CO_2 at the reactor outlet was monitored with an infrared-gas-analyzer (IRGA, "URAS 3G", Hartmann and Braun). All samples were cleaned by heating to above 200 °C for several minutes before the measurements were started.

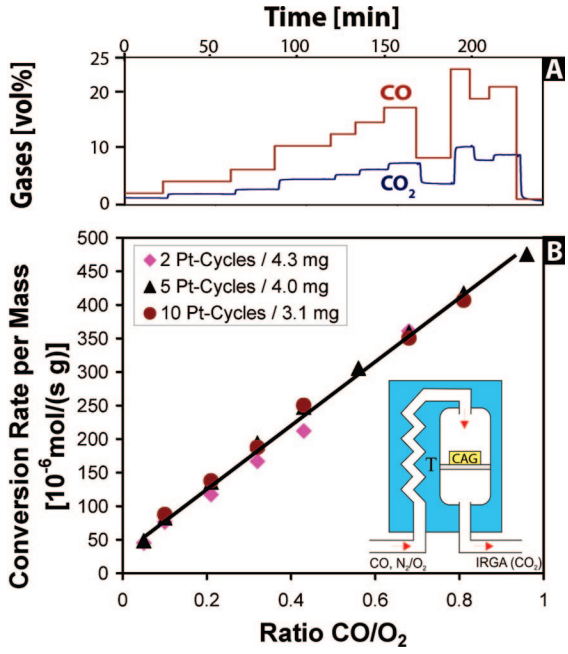

Figure 3. CO oxidation data for Pt-CA nanocomposites. (a) Time series of CO (inlet) and the resulting CO_2 signal at the reactor outlet for 4.0 mg of the 10 ALD cycle Pt-CA. (b) Conversion rate dependence of 2, 5, and 10 ALD cycle Pt-CA on the ratio of CO to O_2 (concentrations at the inlet).

Afterward, nearly full conversion of CO to CO_2 was observed even when temperatures were reduced to 150 °C, whereas, no conversion of CO was observed for undoped CA samples. Figure 3a shows a typical data set collected at 250 °C. The CO_2 concentration measured at the reactor outlet follows the CO concentration as the latter is increased in a stepwise fashion.

The most surprising result is that the activity of the 2 ALD cycle Pt-CA samples was as high as that of the 10 ALD cycle samples. Figure 3b shows conversion rates per gram as the ratio of CO and O_2 was increased. For this experiment, the reactor temperature was held at 250 °C and data was acquired for the 2, 5, and 10 cycle Pt-CA. Using the measured composition of the outlet gas, a conversion rate was calculated, which was then divided by the measured sample mass to yield a conversion rate per gram. Most significantly, the observed conversion rate dependence was found to be sample independent (i.e., the catalytic activity of the sample prepared with two ALD cycles was just as high as that of the sample prepared with ten cycles), indicating that for the conditions used the samples contained an excess of reactive Pt sites. Indeed, we observed that the conversion rate is limited by the thermal stability of the Pt-CA composite material which starts to degrade at a power production of 160 W/g. Furthermore, the linear relationship between conversion rate and the CO/O_2 ratio shown in Figure 3b reveals that the conversion efficiency is near 100%.[19]

To quantify the reaction kinetics, the turnover frequency (TOF) of the Pt-CA catalyst was estimated based on TEM and RBS results. Our analysis is based on the assumptions that (1) the particles have a hemispherical shape and that (2) every surface atom is catalytically active, i.e., an active site. For the two cycle sample this leads to a TOF between 4 s^{-1} and 29 s^{-1} depending on the assumptions made regarding mass transport limitations, that is, full penetration of reactants throughout the cross-section of the Pt-CA versus considering only the outer 10 μm of the material. The latter case appears more reasonable due to the rapid consumption of reactants, independent of the total Pt loading. In any case, the numbers are in good agreement with model experiments.[18] However, the extent of mass transport limitation could not be determined quantitatively on the basis of the present experiments but will be addressed in future studies.

In summary, we have successfully demonstrated the fabrication of catalytically active Pt-loaded CA materials using ALD. Structural analysis of these materials confirmed the growth of discrete crystalline Pt nanoparticles to a depth of >10 μm within the CA support. Excluding some nonideal ALD process close to the surface, the particle size was below 5 nm. RBS analysis showed that the Pt loading in the CAs is extremely low with the areal density of Pt estimated to be ~0.047 mg/cm^2 in the sample prepared with 2 ALD cycles. Remarkably, even at such low loading levels, these materials exhibited high catalytic activity. Carbon monoxide oxidation studies demonstrated near 100% conversion of CO to CO_2 at temperatures ranging from 150 to 250 °C with stability up to a power production of 160 Wg^{1-} (6×10^{-4} mol g^{-1} s^{-1} at 250 °C). For the case of the 2 ALD cycle Pt-CA sample, the turnover frequency lies in the range of 4−29 s^{-1} depending on the assumptions made on mass transport. The technique demonstrated here can be applied to the design of new catalytic materials for a variety of applications, including fuel cells, hydrogen storage, pollution control, green chemistry, and liquid fuel production.

Acknowledgment. S.F.B. acknowledges the Global Climate and Energy Project at Stanford University and the donors of The American Chemical Society Petroleum Research Fund for support. Work at LLNL was performed under the auspices of the U.S. DOE by LLNL under Contract DE-AC52−07NA27344.

References

(1) Bell, A. T. *Science* **2003**, *299*, 1688.
(2) Campbell, C. T. *Science* **2004**, *306*, 234.
(3) Raimondi, F.; Scherer, G. G.; Kotz, R.; Wokaun, A. *Angew. Chem., Int. Ed.* **2005**, *44*, 2190.
(4) Wang, G. X.; Sun, G. Q.; Zhou, Z. H.; Liu, J. G.; Wang, Q.; Wang, S. L.; Guo, J. S.; Yang, S. H.; Xin, Q.; Yi, B. L. *Electrochem. Solid State* **2005**, *8*, A12.
(5) Liu, H. S.; Song, C. J.; Zhang, L.; Zhang, J. J.; Wang, H. J.; Wilkinson, D. P. *J. Power Sources* **2006**, *155*, 95.
(6) Du, H. D.; Gan, L.; Li, B. H.; Wu, P.; Qiu, Y. L.; Kang, F. Y.; Zeng, Y. Q. *J. Phys. Chem. C* **2007**, *111*, 2040.
(7) Saquing, C. D.; Kang, D.; Aindow, M.; Erkey, C. *Microporous Mesoporous Mater.* **2005**, *80*, 11.
(8) Kucheyev, S. O.; Biener, J.; Wang, Y. M.; Baumann, T. F.; Wu, K. J.; van Buuren, T.; Hamza, A. V.; Satcher, J. H.; Elam, J. W.; Pellin, M. J. *Appl. Phys. Lett.* **2005**, *86*, 083108.
(9) Baumann, T. F.; Biener, J.; Wang, Y. M. M.; Kucheyev, S. O.; Nelson, E. J.; Satcher, J. H.; Elam, J. W.; Pellin, M. J.; Hamza, A. V. *Chem. Mater.* **2006**, *18*, 6106.
(10) Biener, J.; Baumann, T. F.; Wang, Y. M.; Nelson, E. J.; Kucheyev, S. O.; Hamza, A. V.; Kemell, M.; Ritala, M.; Leskelä, M. *Nanotechnology* **2007**, *18*, 055303.

(11) Kucheyev, S. O.; Biener, J.; Baumann, T. F.; Wang, Y. M.; Hamza, A. V.; Li, Z.; Lee, D. K.; Gordon, R. G. *Langmuir* **2008**, *24*, 943.
(12) Elam, J. W.; Xiong, G.; Han, C. Y.; Wang, H. H.; Birrell, J. P.; Welp, U.; Hryn, J. N.; Pellin, M. J.; Baumann, T. F.; Poco, J. F.; Satcher, J. H. *J. Nanomaterials* **2006**, 64501.
(13) Leskelä, M.; Ritala, M. *Angew. Chem., Int. Ed.* **2003**, *42*, 5548.
(14) Baumann, T. F.; Worsley, M. A.; Han, T. Y.; Satcher, J. H. *J. Non-Cryst. Solids* **2008**, *354*, 3513.
(15) Aaltonen, T.; Ritala, M.; Sajavaara, T.; Keinonen, J.; Leskelä, M. *Chem. Mater.* **2003**, *15*, 1924.
(16) Xue, Z.; Thridandam, H.; Kaesz, H. D.; Hicks, R. F. *Chem. Mater.* **1992**, *4*, 162.
(17) Doolittle, L. R. *Nucl. Instrum. Methods Phys. Res., Sect. B* **1985**, *9*, 344.
(18) Santra, A. K.; Goodman, D. W. *Electrochim. Acta* **2002**, *47*, 3595.
(19) It should be noted that the sample did not fill the area of the frit, thus a portion of the gas stream by-passed the sample; this was the case especially during measurements where smaller amounts of catalyst were used.

NL801299Z